Comprehensive Analysis of Competitive Endogenous Rnas Network Associated With Hepatocellular Carcinoma

jiahui Wan
Mudanjiang Medical University
Xiuli Wang
Mudanjiang Medical University
Fusheng Zhao
Mudanjiang Medical University
Ying Jiang
Mudanjiang Medical University
Wei Ma
Mudanjiang Medical University
Shijun Jiang
Mudanjiang Medical University
Zikang He
Mudanjiang Medical University
Xiaojin Wang
Mudanjiang Medical University
Rongjun Cui (cuirongjun@mdjmu.edu.cn)
https://orcid.org/0000-0002-8138-168X

Primary research

Keywords: hepatocellular carcinoma, competitive endogenous RNAs, MYLK-AS1, miR-424-5p, CCNE1

Posted Date: August 14th, 2020

DOI: https://doi.org/10.21203/rs.3.rs-58143/v1

Abstract

Background: Increasing evidences show that long non-coding RNA (lncRNA) plays the role of competitive endogenous RNAs (ceRNAs) in the development and progression of cancers. The purpose of our study was to identify potential lncRNA biomarkers that serve as a therapeutic target and prognostic biomarker in HCC.

Methods: The differential expression of RNAs was examined using the edgeR package. Gene ontology (GO) and Kyoto Encyclopedia of Genes and Genomes (KEGG) pathway enrichment analysis were used to predict potential functions. Survival analysis and ROC curve analysis were performed to predict ceRNA network had significant prognostic value. The biological functions of MYLK-AS1 on HCC cells were studied by RNA interference approaches in vitro. Cell proliferation, migration and invasion were detected by Cell Counting Kit-8(CCK-8) assay, wound healing and transwell assay relatively. The mechanism of competitive endogenous RNAs (ceRNAs) were predicted and verified by bioinformatic analysis, western blot analysis and luciferase assays.

Results: The newly constructed ceRNA network comprised 76 HCC specific lncRNAs, 15 miRNAs, and 35 mRNAs from the database (Targetscan, miRTarBase, and miRDB). 10 differentially expressed lncRNAs and 10 differentially expressed mRNAs were significantly associated with overall survival in HCC (*P* value < 0.05). Gene ontology (GO) and Kyoto Encyclopedia of Genes and Genomes(KEGG) pathways enrichment analysis results showed the differentially expressed mRNAs were involved primarily in the most significant cancer-related signaling pathways. ROC curve analysis demonstrated that MYLK-AS1—has-mir-424—CCNE1 ceRNA network had significant prognostic value. The expression of MYLK-AS1 was up-regulated in HCC cells and tissues. Biological function analyses indicated that down-regulation of MYLK-AS1 suppressed cell proliferation, migration and invasion . MYLK-AS1 and miR-424-5p bound directly and reversibly to each other. MYLK-AS1 could positively regulate CCNE1 expression by competitively binding to miR-424-5p.

Conclusion: The current study provides novel insights into the lncRNA-related ceRNA network in HCC and the MYLK-AS1 may be a candidate biomarker for molecular diagnosis and prognosis monitoring of HCC.

Introduction

Hepatocellular carcinoma (HCC) is a kind of malignant tumor with high morbidity and mortality[1-2]. More than 70% of new cases of HCC occur in Asia each year, and more than 50% of these new cases occur in China[3]. The treatment and adverse reactions of HCC have always been global challenges. Therefore, the search for early diagnostic markers and more effective and safer treatments are significance for improving the clinical strategies and prognosis of HCC. LncRNAs are transcripts of more than 200 nucleotides that have been shown to be involved in a variety of biological processes such as chromosomal silencing[4], chromatin modification[5], transcriptional activation[6] and transcriptional interference[7]. There is continuous evidence that lncRNAs can participate in a variety of physiological

and pathological processes in human cancer, affecting cell proliferation, migration and invasion. For example, LncRNA-HOST2 can promote cell proliferation, migration and invasion and inhibit cell apoptosis in human HCC cell line SMMC-7721[8]; LncRNA WWOX-AS1 inhibits the proliferation, migration and invasion of osteosarcoma cells[9]; Lnc-MMP2-2 might regulate the migration and invasion of lung cancer cells into the vasculature by promoting MMP2 expression, suggesting this lncRNA as a novel therapeutic target and predictive marker of tumor metastasis in lung cancer[10]; Long non-coding RNA lnc-GNAT1-1 inhibits gastric cancer cell proliferation and invasion through the Wnt/β-catenin pathway in Helicobacter pylori infection[11].

LncRNA acts as a competitive endogenous RNA (ceRNA) that binds to microRNAs (miRNAs) to regulate its downstream target genes[12-15] . At the same time, miRNA is an important regulator of HCC tumorigenesis and development. miR-199a-3p regulates MTOR and PAK4 pathways and inhibits tumor growth in hepatocellular carcinoma, miR-199a-3p may be promising as an HCC treatment option[16]. APA Zekri, A. N. et al. identified a miRNA panel comprised of four miRNAs (miR-192, miR-122, miR-181b and miR-125a-5p) that may serve as a molecular tool for characterization of the CD133+ cells associated with different stages of hepatocarinogensis[17]. MiR-18a may serve as a prognostic biomarker of HCC as it is demonstrated to carry out a decisive role in HCC progression by promoting HCC cell invasion, migration, and proliferation through targeting Bcl2L10[18].

In present research was based on TCGA, we analyzed the RNA expression profiles from 374 tumors and 50 adjacent normal tissues in HCC. As a result, 1082 differentially expressed lncRNAs (DElncRNAs), 122 differentially expressed miRNAs (DEmiRNAs) and 1992 differentially expressed mRNAs (DEmRNAs) were identified in our study. In order to elucidate the interactions and valid potential crosstalk between RNAs, we successfully established the HCC associated ceRNA network based on bioinformatics generated from Targetscan, miRTarBase, and miRDB, which included 76 lncRNAs, 15 miRNAs and 35mRNAs. Furthermore, genes of ceRNA network were analyzed for overall survival to identify prognostic genes with clinical characteristics. In addition, we identified MYLK-AS1 regulated tumorigenesis of HCC. We found that MYLK-AS1 was markedly upregulated in HCC cells. Knocking down MYLK-AS1 could inhibit HCC cell proliferation and migration via functioning as a ceRNA for miR-424-5p, thereby preventing its association with CCNE1. Collectively, the results showed that MYLK-AS1 is a novel tumor biomarker that can be used as a potential target for clinical diagnosis and treatment of HCC.

Materials And Methods

Patients and samples from the TCGA database

To search the specific of lncRNAs, miRNAs and mRNAs in HCC, we downloaded gene expression data from the TCGA database (https://portal.gdc.cancer.gov/, up to April 9, 2020, including 374 HCC tissues and 50 adjacent normal tissues).

RNA sequence data processing and differential expression analysis

The differentially expressed mRNAs (DEmRNAs), lncRNAs (DElncRNAs) and miRNAs (DEmiRNAs) between the HCC tissues and adjacent normal tissues was identified by EdgeR package in R (version 3.4.1), and $P < 0.01$ and $|logFC| > 2$ were set as the cut-off criteria. The ggplot2 packages in R were used to visualize volcano plots.

Establishment of the ceRNA network

The miRcode online tool (http://www.mircode.org) were used to predict DElncRNAs-DEmiRNAs interactions in HCC. Furthermore, The miRDB (http://www.mirdb.org), miRTarBase (http://mirtarbase.mbc.nctu.edu.tw), and Targetscan (http://www.targetscan.org) database were used to predict the DEmRNAs targeted by DEmiRNAs. Finally, ceRNA networks was established by DEmiRNAs that regulate expression of DEmRNA and DElncRNA, DElncRNAs-DEmiRNAs-DEmRNAs ceRNA network were visualized by Cytoscape (version 3.5.1).

Functional enrichment analysis

GO enrichment analysis were performed with the Database for Annotation, Visualization and Integrated Discovery (DAVID, https://david.ncifcrf.gov/), $P<0.05$ was set as the cut-off criterion. KEGG pathway analysis were performed with packages in R, the threshold was $P<0.05$, R clusterProfiler package were used to predict potential functions for the DEmRNAs in the ceRNA network.

Human HCCtissues and adjacent normal tissues microarray

The expression of MYLK-AS1 was detected by human HCC tissue and adjacent normal tissue microarrays (Lnc cDNA-HLivH090Su01, OUTDO BIOTECH, Shanghai, China). These tissue microarrays included 64 cases and 26 HCC tissues and adjacent normal tissues, respectively. The Taizhou Hospital Ethics Committee of Zhejiang Province authorized all experiments in patient organizations in this study and obtained informed consent from each patient participating in the study.

Cell culture

Human liver cancer cell lines (Huh7 and HepG2) and normal liver epithelial cell line (LO2) were obtained from the Chinese Cell Bank of the Chinese Academy of Sciences (Shanghai, China). All cells were cultivated in Dulbecco modified Eagle medium (DMEM) together with 10% fetal bovine serum (FBS; Gibco Waltham, MA), 100U/mL penicillin as well as 100μg/mL streptomycin (both from Sigma-Aldrich, St Louis, MO) in a humidified temperature at 37°C with 5% CO2

RNA extraction and real-time PCR analysis

Total RNAs were extracted from cells using RNAiso Plus (TaKaRa, Tokyo, Japan). A reverse transcription kit (RR036A; TaKaRa) was used to transcribe total RNA and produce complementary DNA (cDNA). Real-time PCR was performed with SYBR Premix Ex Taq II (TaKaRa) and NanoDrop 2000c (Thermo Scientific, Waltham, MA, USA). Expression of genes was normalized to that of glyceraldehyde 3-phosphate

dehydrogenase (GAPDH) or U6. Relative RNA expressions were measured with ABI Prism 7500 Software v2.0.6 (Thermo Fisher Scientific, Waltham, MA) and calculated

based on the $2^{-\Delta\Delta C\,t}$ method.

Western blot analysis

Proteins were isolated from tissues by lysing frozen tissues in radioimmunoprecipitation assay (RIPA) buffer (Sigma-Aldrich). Equal amounts of protein (50 μg) were separated by 12% sodium dodecyl sulfate polyacrylamide gel electrophoresis (SDS PAGE) and transferred to a polyvinylidene fluoride (PVDF) membrane (Thermo Fisher Scientific, Billerica, MA). The membrane was blocked with 5% bovine serum albumin (BSA) overnight and incubated with primary antibodies including CCNE1 and GAPDH (Cell Signaling Technology). GAPDH was used as an internal control. Protein bands were visualized by the enhanced chemiluminescence (ECL) detection system (Applygen Technologies, Beijing, China).

Cell proliferation assay

The cell suspension (100 μL/well) was seeded in a 96-well plates. The plate was pre-incubated in an incubator (at 37 °C, 5% CO^2). Add 10 μL of CCK-8 solution to each well. Incubate the plates in the incubator for 24, 48, 72, 96 hours. The absorbance at 450 nm was measured with a microplate reader.

Colony formation assay

Huh7 and HepG2 cells were trypsinized to make a single cell suspension, 500 cells were inoculated into each well and the medium was changed every three days. Culture was stopped after 3 weeks, the cells were washed with phosphate-buffered saline (PBS), fixed with methanol and stained with crystal violet (Sinopharm Chemical Reagent, Beijing, China). The colonies were counted under a fluorescence microscope (Olympus Corporation, Tokyo, Japan).

Wound healing assay

The marker pen draws a horizontal line evenly behind the 6-well plates (Corning), with a horizontal line every 0.5 ~ 1.0 cm. 5×10^5 cells were seeded into to the well. Cell scratch line perpendicular to the horizontal line was made using a 200 μL pipette tip. 6-well plates were incubated in the incubator(at 37 °C, 5% CO^2). The sample was taken out and photographed at 0, 24 hours.

Transwell invasion assay

5×10^4 cells/200 ul of serum-free cell suspension was added to the Matrigel Invasion Chambers (size 8 μm; BD Biosciences, Franklin Lakes, NJ, USA), 600 μL of medium containing 10% FBS was added to the lower chamber of 24-well plates (Corning). Continue to cultivate for 24 hours, the chamber was removed and the phosphate-buffered saline (PBS) were used to wash the cells twice, the cells were fixed in

methanol, and the cells were stained with crystal violet. The cells were observed, and were counted 5 fields of view under the microscope (Olympus, Tokyo, Japan).

Dual luciferase reporter assay

Wild plasmids was constructed by cloning into the psi-CHECK-2 vector (Promega, Madison, WI, USA) using XhoI and NotI sites. Mutant plasmids were generated using the QuickChange® Site-Directed Mutagenesis kit (Stratagene, Agilent Technologies, Wilmington, DE, USA). The appropriate plasmid and miR-424-5p mimic or mimic control were co-transfected into HEK293T cells (1.0×10^5), and the luciferase assay was evaluated 48 hours after transfection using the Dual-luciferase Reporter Assay System (Promega). Renilla luciferase activity was used for standardization.

Statistical analysis

The clinical data on the patients were combined with HCC data in TCGA to evaluate the prognostic value of differential RNAs in the ceRNA network. Survival curves were generated using the survival package in R for samples with differentially expressed mRNAs and lncRNAs. All results presented as the mean ± standard deviation (S.D.). Oneway analysis of variance (ANOVA) was used to examine statistical comparisons among groups. Two-tailed Student's t-test was performed to compare the means of values from different experiments. Differences were considered statistically significant if $P < 0.05$. All statistical analyses were performed using GraphPad Prism 5.0 (GraphPadSoftware, Inc., La Jolla, CA, USA). Each experiment was performed for three times.

Results

Identifying DEmRNAs, DEmiRNAs, and DElncRNAs in HCC

The RNA expression profiles of patients with HCC and corresponding clinical information were downloaded from the TCGA database using the Data Transfer Tool. We used EdgeR to identify significantly DEmRNAs, DEmiRNAs, and DElncRNAs between HCC tissues and adjacent normal tissues. This identified a total of 1992 DEmRNAs, 122 DEmiRNAs, and 1082 DElncRNAs. More specifically, there were 1787 (89.7%) up-regulated and 205 (10.3%) down-regulated DEmRNAs (Table S1), 119 (97.5%) up-regulated and 3 (2.5%) down-regulated DEmiRNAs (Table S2), and 58 (5.4%) down-regulated DElncRNAs and 1024 (94.6%) up-regulated DElncRNAs identified (Table S3). A heat map demonstrating the complete linkage clustering of DEmRNAs, DEmiRNAs, and DElncRNAs is shown in Fig. 1.

Predictions of mRNAs and lncRNAs targeted by miRNAs

Next, we predicted the mRNAs and lncRNAs that were targeted by miRNAs, focusing on the relationship the 122 differentially expressed miRNAs and 1082 differentially expressed lncRNAs above. Only 15 of 122 differentially expressed miRNAs were predicted to target 76 of 1082 differentially expressed lncRNAs (table1). The relationships between these 15 differentially expressed lncRNA-targeting miRNAs were used

to predict the targeted mRNAs using Targetscan, miRTarBase, and miRDB. Then, 15 HCC-specific miRNAs were predicted to target the 35 mRNAs (table2).

Table1. 15 DEmiRNAs interact with the 76 DElncRNAs

miRNA	LncRNA
hsa-mir-424	MYLK-AS1 C2orf48 CCDC13-AS1 AL033381.1 AP002478.1 FAM87A WT1-AS TCL6 AC087392.1 AC006305.1 AC016773.1 LINC00473 WARS2-IT1 SFTA1P LINC00355 LINC00200 LINC00160 DLX6-AS1 BPESC1 DSCR10 TSPEAR-AS1 GPC6-AS1 CLRN1-AS1 PART1 HOTTIP GDNF-AS1 PVT1 RMST LINC00485
hsa-mir-519d	C2orf48 AP002478.1 FAM87A WT1-AS LINC00308 LINC00221 TCL6 AC087392.1 AC061975.6 AL512652.1 TDRG1 AL359878.1 AC006305.1 HOTAIR LINC00200 DLX6-AS1 LINC00462 SRGAP3-AS4 HOTTIP PVT1 GRM5-AS1 RMST AC040173.1
hsa-mir-217	AL357153.1 AC024563.1 WT1-AS LINC00221 TCL6 AC016773.1 HOTAIR LINC00200 MIR137HG LINC00494 CLRN1-AS1 MYLK-AS1 AP000553.1 CRNDE PVT1 AC040173.1 NOVA1-AS1
hsa-mir-182	AP002478.1 WT1-AS LINC0022 TCL6 AC006305.1 AL163952.1 ZNF385D-AS2 LINC00114 SFTA1P ERVMER61-1 MIR137HG ERVH48-1 LINC00494 MYLK-AS1 AC012640.1 AC073352.1 GRM5-AS1 RMST AC040173.1
hsa-mir-506	AL033381.1 FAM87A LINC00221 LINC00501 AL359878.1 AC006305.1 LINC00355 HOTAIR LINC00200 SACS-AS1 ERVMER61-1 DLX6-AS1 BPESC1 LINC00316 MYLK-AS1 HOTTIP PVT1 RMST
hsa-mir-183	C2orf48 AL357153.1 AC024563.1 TCL6 LINC00501 LINC00392 LINC00200 CRNDE PVT1 AC040173.1
hsa-mir-96	FAM87A WT1-AS LINC00221 TCL6 AL163952.1 LINC00488 ZNF385D-AS2 LINC00114 ERVMER61-1 ERVH48-1 AC073352.1 GRM5-AS1 RMST AC040173.1
hsa-mir-373	C2orf48 AC009065.1 AP002478.1 C10orf91 WT1-AS LINC00221 TCL6 AC087392.1 AC061975.6 AL359878.1 SACS-AS1 DLX6-AS1 LINC00462 LINC00494 LINC00322 HOTTIP PVT1 GRM5-AS1 LINC00485
hsa-mir-372	C2orf48 AC009065.1 AP002478.1 C10orf91 WT1-AS LINC00221 TCL6 AC087392.1 AC061975.6 AL359878.1 SACS-AS1 DLX6-AS1 LINC00462 LINC00494 LINC00322 HOTTIP PVT1 GRM5-AS1 LINC00485
hsa-mir-141	PART1 CCDC13-AS1 AL357153.1 AC024563.1 FAM87A WT1-AS LINC00308 AL512652.1 AL359878.1 LINC00355 AL713998.1 CCDC26 DLX6-AS1 BPESC1 ERVH48-1 AC009121.1 MYLK-AS1 AC114489.1 HOTTIP LINC00485
hsa-mir-137	LINC00308 TCL6 AC006305.1 AC073263.1 CLDN10-AS1 HTR2A-AS1 AL713998.1 ERVH48-1 GPC6-AS1 CLRN1-AS1 AC012640.1 HOTTIP RMST
hsa-mir-205	PART1 CCDC13-AS1 AP002478.1 FAM87A LINC00308 TCL6 AL512652.1 AL163952.1 LINC00488 ZNF385D-AS1 LINC00351 CCDC26 SACS-AS1 ERVMER61-1 BPESC1 GPC6-AS1 CLRN1-AS1 MYLK-AS1 AC012640.1 HOTTIP AC011453.1 CRNDE PVT1 GRM5-AS1 RMST LINC00485
hsa-mir-216a	C2orf48 AP002478.1 TCL6 AC087392.1 AL359878.1 AC006305.1 LINC00488 AL357060.1 AC016773.1 LINC00114 WARS2-IT1 SFTA1P HOTAIR LINC00200 DLX6-AS1 BPESC1 AL589947.1 CLRN1-AS1 MYLK-AS1 HOTTIP GDNF-AS1 PVT1 NOVA1-AS1 LINC00485 LINC00519
hsa-mir-184	AP002478.1 ERVH48-1 TSPEAR-AS1 HOTTIP LINC00491

hsa-mir-216b	FAM87A WT1-AS TCL6 AL163952.1 LINC00488 WARS2-IT1 SFTA1P HOTAIR LINC00200 DLX6-AS1 BPESC1 CLRN1-AS1 AC012640.1 CRNDE PVT1 LINC00491 GRM5-AS1 NOVA1-AS1

Table2. 15 DEmiRNAs interact with the 35 DEmRNAs

miRNA	mRNA
hsa-mir-424	CCNE1 CDC25A AXIN2 E2F7 CEP55 KIF23 CBX2 HOXA10 GNAL HOXA3 ITGA2 CLSPN CPEB3
hsa-mir-519d	KIF23 E2F2 NETO2 E2F1 ELAVL2 POLQ RRM2 SALL3 ACSL4
hsa-mir-217	EZH2 DACH1
hsa-mir-182	NPTX1 FOXF2 HOXA9
hsa-mir-506	LRRC1 ZWINT
hsa-mir-183	GLUL CCNB1
hsa-mir-96	PROK2
hsa-mir-373	ELAVL2 SLC7A11 PBK
hsa-mir-372	SLC7A11 ELAVL2
hsa-mir-141	ELAVL2 EPHA2
hsa-mir-137	PTGS2
hsa-mir-205	ACSL4
hsa-mir-216a	NOM1 LAMC1 PAK1 FAM117B TGFBR2 SP4 MYLIP GPBP1 MTO1 TWISTNB OXGR1
hsa-mir-184	LRRC8A
hsa-mir-216b	PPP2CB COL4A4 TM9SF3 ZDHHC9 SMAD1 TPM3 KLF12 CCDC65 DNAJB9 ZNF566 C11orf57 AKIP1 SOCS6 ARL6IP1 FZD5 MCM4

Construction of the ceRNA network

To reveal how lncRNA may mediate transcription in HCC by affecting mRNA and miRNA binding, a ceRNA network based on the lists of DElncRNAs, DEmiRNAs, and DEmRNAs was constructed and visualized using Cytoscape software. As shown in Fig. 2, the lncRNA-miRNA-mRNA network was comprised of 15 miRNA nodes, 35 mRNA nodes, 76lncRNA nodes.

Survival analysis with differentially expressed lncRNAs and mRNAs

To investigate the relationship between the differentially expressed lncRNAs and mRNAs and the prognosis of HCC patients, the Kaplan–Meier method was used to analyze the relationship between the differential expression of 76 lncRNAs and 35 mRNAs and the overall survival rate in HCC patients. The most significant 10 of 77 differentially expressed lncRNAs were associated with the prognosis in HCC: MYLK-AS1, AL163952.1, ERVMER61-1, WARS2-IT1, AC073352.1, HTR2A-AS1, CLRN1-AS1, AL359878.1, C10orf91, AP002478.1 (log-rank $P < 0.05$) (Fig. 3). The most significant 10 of 35 differentially expressed mRNAs were linked to the prognosis in HCC: CCNE1, NPTX1, CPEB3, E2F2, RRM2, KIF23, E2F7, CDC25A CCNB1, E2F1 (log-rank $P < 0.05$) (Fig. 4).

Functional enrichment analysis based on mRNAs

To establish context of ceRNA network, we inferred the roles of each lncRNA based on the functions of connected mRNAs. lncRNAs were typically central and connected to one or more mRNAs in the network. The top 16 highly enriched GO terms of biological process (BP), cellular component (CC) and molecular function (MF). GO analysis was conducted to ascertain the signaling cascade that the 25 genes participate(Fig. 5). Finally, KEGG pathway analysis revealed that 9 pathways were significantly enriched, particularly mRNAs involved in cancer(Fig. 6).

Prognostic value of MYLK-AS1—has-mir-424—CCNE1 ceRNA network

ROC curves were constructed to evaluate the sensitivity and specificity of MYLK-AS1—has-mir-424—CCNE1 ceRNA network for prediction of HCC diagnosis. The area under the ROC curve of MYLK-AS1, has-mir-424 and CCNE1 was 0.91, 0.97 and 0.95 respectively. (Fig. 7A-C). To investigate whether MYLK-AS1 correlated with CCNE1 in HCC, we performed expression analysis and found a positive correlation between MYLK-AS1 and CCNE1 expression in HCC using TCGA database [19](Fig.7D)

Differential expression of MYLK-AS1 in HCC cells and tissues

In our study, Our results showed that MYLK-AS1 expression was significantly increased in two HCC cell lines (Huh7, HepG2) compared with that in normal HCC epithelial cell line LO2 (Fig.8A).MYLK-AS1 expression was higher in HCC tissues than adjacent normal tissues by human HCC tissue and adjacent normal tissue microarrays. (Fig.8B, C). In addition, MYLK-AS1 expression was further analysed according to patients' clinical pathological features. Higher expression of MYLK-AS1 correlated with larger tumour

size, advanced TNM stage (Fig.8D, E). The area under the ROC curve of MYLK-AS1 was 0.75(Fig.8F). Kaplan-Meier survival analysis and log-rank tests showed that higher MYLK-AS1 expression was associated with shorter survival time (Fig. 8G). Collectively, these findings indicate that MYLK-AS1 is a potential biomarker for diagnosis and prognosis in HCC.

MYLK-AS1 silencing inhibits HCC cells proliferation,migration and invasion

To examine the biological functions of MYLK-AS1, the si-MYLK-AS1 1#, si- MYLK-AS1 2#, si-MYLK-AS1 3#, or si negative control (NC) were separately transfected into Huh7 and HepG2 cells. We found that MYLK-AS1 expression was remarkably reduced in si-MYLK-AS1 3# transfected into HCC cells compared with si NC (Fig. 9A). The CCK8 assay and plate clone formation assay was used to determine the role of MYLK-AS1 in cell growth. In Huh7 and HepG2 cells, MYLK-AS1 knockdown led to reduced cell proliferation compared with that observed in the si NC cells (Fig. 9B, C). Furthermore, in the wound healing assay, knockdown of MYLK-AS1 contributed to slower scratch healing (Fig. 9D). Transwell assay revealed that the invasion ability of cells in which MYLK-AS1 was silenced was suppressed compared with that of si NC (Fig.9E). These results reported that MYLK-AS1 could promote the proliferation and metastasis of HCC cells.

MYLK-AS1 functions as a ceRNA and sponges miR-424-5p in HCC cells.

To investigate the molecular mechanism by which MYLK-AS1 acting as ceRNAs. First of all, MYLK-AS1 knockdown significantly increased the expression level of miR-424-5p (Fig. 10A), This finding suggested that MYLK-AS1 may function as a ceRNA of miRNAs. To determine this hypothesis, We then performed dual luciferase reporter assays to confirm the prediction analysis. HEK293T cells were transfected with a luciferase plasmid harboring the sequence of MYLK-AS1 together with plasmids encoding the miRNAs or a control sequence. We found that miR-424-5p could suppress MYLK-AS1-driven luciferase activity, and the suppression ability of miR-424-5p is stronger (Fig. 10B). To determine whether miR-424-5p functions as a tumor suppressor in HCC cells, we transfected Huh7 and HepG2 cells with miR-424-5p mimic or inhibitor (Fig. 10C). Real-time PCR analysis confirmed that the expression of MYLK-AS1 was lower in miR-424-5p mimic compared with mimic control, the expression of MYLK-AS1 was higher in miR-424-5p inhibitor compared with inhibitor control(Fig. 10D). We then performed CCK-8 and colony formation found that cell proliferation and colony formation ability were significantly reduced by overexpression of miR-424-5p (Fig. 10E,F)and significantly enhanced by silencing of miR-424-5p expression (Fig.11A,B). the wound healing assay and transwell assay found that cell migration and invasive ability were significantly reduced by overexpression of miR-424-5p (Fig. 10G,H) and significantly enhanced by silencing of miR-424-5p expression (Fig.11C,D)

CCNE1 is a miR-424-5p target gene and is indirectly regulated by MYLK-AS1

To determine the ceRNA network between MYLK-AS1, miR-424-5p and its targets in HCC. We found that knockdown of MYLK-AS1 also significantly reduced CCNE1 mRNA and protein levels in Huh7 and HepG2 cells (Fig. 12A). To determine whether CCNE1 is regulated by miR-424-5p liver cancer cells, we measured

CCNE1 mRNA and protein levels when miR-424-5p was over-expressed or inhibited in Huh7 and HepG2 cells. We found that CCNE1 mRNA and protein levels were significantly decreased by miR-424-5p overexpression (Fig. 12B), in contrast, CCNE1 mRNA and protein levels were significantly increased by miR-424-5p inhibition (Fig. 12C). Nest, we performed luciferase reporter assays driven by the wild-type 3' UTR sequence of CCNE1, which contains the predicted miR-424-5p binding site (wt- CCNE1), or mutant constructs containing a mutation in the miR-424-5p-binding sites (mut- CCNE1). These plasmids were co-transfected into HEK293T cells together with miRNA mimic control or miR-424-5p mimic. The results showed that wt- CCNE1-driven luciferase expression was significantly reduced by co-transfection with the miR-424-5p mimic compared with the control, but this repression was abolished by mutation of the putative miR-424-5p-binding site in the CCNE1 3'UTR (Fig. 12D). Taken together, these results indicate that miR-424-5p regulates CCNE1 expression in liver cancer cells by directly binding to the predicted site in the 3' UTR of CCNE1 mRNA.

miR-424-5p plays a role in the relationship between MYLK-AS1and CCNE1

To determine whether miR-424-5p is involved in mediating the effects of MYLK-AS1 in HCC cells, Huh7 and HepG2 cells were co-transfected with si- MYLK-AS1 3# and miR-424-5p inhibitor. Notably, In addition, proliferation and colony forming assays revealed that inhibition of the miR-424-5p promoted the proliferation of Huh7 and HepG2 cells, and this effect was partly reversed by co-transfection with si-MYLK-AS1 3# (Fig. 13A and B), the wound healing assay and transwell invasion assay found that was partially rescued by co-transfection with miR-424-5p inhibitor(Fig. 13C and D). To determine whether miR-424-5p plays a role in the relationship between si-MYLK-AS1 3# and CCNE1, we examined cells co-transfected with si-MYLK-AS1 3# and the miR-424-5p inhibitor. Indeed, the suppression of CCNE1 protein levels induced by si-MYLK-AS1 3# was effectively reversed by the miR-424-5p inhibitor(Fig. 13E). Collectively, these data suggest that MYLK-AS1 modulates the expression of CCNE1 by post-transcriptional regulation of miR-424-5p.

Discussion

A large amount of evidence has demonstrated that ceRNA plays an important role of human diseases, including thyroid cancer[20], non-small cell lung cancer[21], and ovarian cancer[22]. However, the role and mechanism of ceRNA in HCC remains unclear.

In this study, RNA sequencing data and the clinical characteristics of HCC were obtained from the Cancer Genome Atlas database. DElncRNAs, DEmRNAs, and DEmiRNAs were identified between HCC and normal HCC tissue samples. Subsequently, the lncRNA-miRNA-mRNA ceRNA network of HCC was established. We identified a novel lncRNA-MYLK-AS1 associated with HCC, which is significantly upregulated in HCC cell lines. This research demonstrated that MYLK-AS1 modulate cell proliferation, migration and invasion in HCC cells. Luciferase reporter assay confirmed that miR-424-5p was a target of MYLK-AS1 in HCC cells. These findings indicated that MYLK-AS1 played an oncogenic role in HCC and could be considered as a potential prognostic indicator for HCC.

Although lncRNA has received extensive attention in recent years, miRNAs also deserves more attention. Undoubtedly, the cancer-related signaling pathways based on miRNAs regulation is indispensable. Misregulated expression miRNAs is reported to play various roles in tumorigenesis. It is reported that miR-424-5p functions as tumor suppressor gene in many cancers. For example, the inhibition of has-mir-424 in SNHG12-depleted cells partially reversed the effects on cervical cancer cell apoptosis, adhesion and invasion [23]. Another report shows that has-mir-424 -SMAD7 pathway contributed to ESCC invasion and metastasis and up-regulation of has-mir-424 perhaps provided a strategy for preventing tumor invasion, metastasis[24]. In this study, we found that miR-424-5p was significantly down-regulated in HCC cells, and miR-424-5p mimic or inhibitor could impair or promote HCC cell proliferation, migration and invasion. Our findings uncover the significance of the interaction between MYLK-AS1 and miR-424-5p in tumorigenesis given that MYLK-AS1 exerts oncogenic behavior partly via sponging miR-424-5p in HCC cells. In addition, miR-424-5p functions as a tumor suppressor and directly targets CCNE1 as potential prognostic markers in epithelial ovarian cancer [25].

The miRNAs-targeted genes involved in ceRNA network were performed the GO term analysis and KEGG pathways enrichment analysis. These genes, E2F2, E2F7, E2F1,CCNE1, CDC25A and KIF23 not only enriched in GO term analysis or KEGG pathway but also included in the ceRNA network. We found that these genes play a key regulatory role in the occurrence and development of tumors[26-30]. Few studies have reported the role of CCNE1 in HCC, so the molecular mechanism of CCNE1 in HCC was also our focus. We conducted luciferase reporter assays and verified that miR-424-5p targeted CCNE1 mRNA at its 3′ UTR. Moreover, miR-424-5p mimic inhibited CCNE1 protein expression, and miR-424-5p inhibitor promoted CCNE1 protein expression. Simultaneously, knockdown of MYLK-AS1 also significantly reduced CCNE1 protein level. Thus, we confirmed CCNE1 as the direct target of miR-424-5p. MYLK-AS1 may act as a ceRNA to regulate the expression of CCNE1 by repressing its inhibitor miR-424-5p.

Conclusion

In summary, we found that some lncRNAs and mRNAs were significantly associated with overall survival in HCC patients. Importantly, we successfully constructed the lncRNA -related ceRNA network, bringing new approach to lncRNA research in HCC, and providing novel lncRNA MYLK-AS1 as candidate prognosis biomarkers or potential therapeutic targets.

Abbreviations

MYLK-AS1: MYLK antisense RNA 1; HCC: hepatocellular carcinoma; CCNE1: cyclin E1; GAPDH: glyceraldehyde phosphate dehydrogenase.

Declarations

Acknowledgment

Not applicable.

Author contributions statement

J.H.W., R.J.C. and X.L.W. wrote the main manuscript text, W.M., Y.J. and X.J.W. prepared all figures. S.J.J., F.S.Z. and Z.K.H. designed the experiments, and all authors reviewed the manuscript.

Funding

This work was supported by grants from the Postgraduate Innovation Research Project of Mudanjiang Medical University (No.2019YJSCX-02MY), Basic scientific research business expenses project of Heilongjiang Provincial Department of Education (2019-KYYWF-0936).

Availability of data and materials

All data supporting the findings of this study are included in this published article.

Ethics approval and consent to participate

Not applicable.

Consent for publication

All authors agreed on the manuscript.

Competing interests

The authors declare that they have no competing interests.

References

1. Bray F, Ferlay J, Soerjomataram I, et al. Global cancer statistics 2018: GLOBOCAN estimates of incidence and mortality worldwide for 36 cancers in 185 countries. CA Cancer J Clin. 2018;68(6):394-424.
2. Siegel RL, Miller KD, Jemal A. Cancer statistics, 2018. CA: a cancer journal for clinicians. 2018; 68(1): 7-30.
3. Ashtari S, Pourhoseingholi MA, Sharifian A, et al. Hepatocellular carcinoma in Asia: Prevention strategy and planning. World J Hepatol. 2015;7(12):1708-17.
4. Pintacuda G, Wei G, Roustan C, et al. hnRNPK Recruits PCGF3/5-PRC1 to the Xist RNA B-Repeat to Establish Polycomb-Mediated Chromosomal Silencing. Mol Cell. 2017;68(5):955-969.e10.
5. Ernst EH, Nielsen J, Ipsen MB, et al.Transcriptome Analysis of Long Non-coding RNAs and Genes Encoding Paraspeckle Proteins During Human Ovarian Follicle Development. Front Cell Dev Biol. 2018;6:78.

6. Shao M, Yang Q, Zhu W, et al. LncHOXA10 drives liver TICs self-renewal and tumorigenesis via HOXA10 transcription activation. Mol Cancer. 2018;17(1):173.
7. Roy B, Wang Q, Dwivedi Y. Long Noncoding RNA-Associated Transcriptomic Changes in Resiliency or Susceptibility to Depression and Response to Antidepressant Treatment. Int J Neuropsychopharmacol. 2018;21(5):461-472.
8. Liu RT, Cao JL, Yan CQ, et al. Effects of LncRNA-HOST2 on cell proliferation, migration, invasion and apoptosis of human hepatocellular carcinoma cell line SMMC-7721. Biosci Rep. 2017;37(2). pii: BSR20160532.
9. Qu G, Ma Z, Tong W, et al. LncRNA WWOX-AS1 inhibits the proliferation, migration and invasion of osteosarcoma cells. Mol Med Rep. 2018;18(1):779-788.
10. Wu DM, Deng SH, Liu T, et al. TGF-β-mediated exosomal lnc-MMP2-2 regulates migration and invasion of lung cancer cells to the vasculature by promoting MMP2 expression. Cancer Med. 2018;7(10):5118-5129.
11. Liu L, Shuai T, Li B, et al. Long non-coding RNA lnc-GNAT1-1 inhibits gastric cancer cell proliferation and invasion through the Wnt/β-catenin pathway in Helicobacter pylori infection. Mol Med Rep. 2018;18(4):4009-4015.
12. Wu Y, Zhang L, Zhang L, et al. Long non-coding RNA HOTAIR promotes tumor cell invasion and metastasis by recruiting EZH2 and repressing E-cadherin in oral squamous cell carcinoma[J]. Int J Oncol, 2015, 46(6):2586-2594.
13. Ao X, Jiang M, Zhou J, Liang H, Xia H, Chen G. lincRNA-p21 inhibits the progression of non-small cell lung cancer via targeting miR-17-5p. Oncol Rep. 2019;41(2):789-800.
14. Li J, Zhang Z, Xiong L, et al. SNHG1 lncRNA negatively regulates miR-199a-3p to enhance CDK7 expression and promote cell proliferation in prostate cancer [J]. Biochem Biophys Res Commun, 2017, 487(1):146-152.
15. Chen Z, Zhen M, Zhou J. LncRNA BRE-AS1 interacts with miR-145-5p to regulate cancer cell proliferation and apoptosis in prostate carcinoma and has early diagnostic values[J]. Biosci Rep, 2019, pii: BSR20182097.
16. Callegari E, D'Abundo L, Guerriero P, et al. miR-199a-3p Modulates MTOR and PAK4 Pathways and Inhibits Tumor Growth in a Hepatocellular Carcinoma Transgenic Mouse Model. Mol Ther Nucleic Acids. 2018;11:485-493.
17. Zekri AN, El-Sisi ER, Youssef ASE, et al. MicroRNA Signatures for circulating CD133-positive cells in hepatocellular carcinoma with HCV infection. PLoS One. 2018;13(3):e0193709.
18. Wang X, Lu J, Cao J, et al. MicroRNA-18a promotes hepatocellular carcinoma proliferation, migration, and invasion by targeting Bcl2L10. Onco Targets Ther. 2018;11:7919-7934.
19. Tang Z, Li C, Kang B, Gao G, Li C, Zhang Z. GEPIA: a web server for cancer and normal gene expression profiling and interactive analyses. Nucleic Acids Res 2017, 45,W98-W102, 10.1093/nar/gkx247.

20. Zhang H, Cai Y, Zheng L, et al. Long noncoding RNA NEAT1 regulate papillary thyroid cancer progression by modulating miR-129-5p/KLK7 expression. J Cell Physiol. 2018;233(10):6638-6648.
21. Liu L, Zhou XY, Zhang JQ, et al. LncRNA HULC promotes non-small cell lung cancer cell proliferation and inhibits the apoptosis by up-regulating sphingosine kinase 1 (SPHK1) and its downstream PI3K/Akt pathway. Eur Rev Med Pharmacol Sci. 2018;22(24):8722-8730.
22. Yao N, Yu L, Zhu B, Gan HY, Guo BQ. LncRNA GIHCG promotes development of ovarian cancer by regulating microRNA-429. Eur Rev Med Pharmacol Sci. 2018;22(23):8127-8134.
23. Dong J, Wang Q, Li L, et al. Upregulation of Long Non-Coding RNA Small Nucleolar RNA Host Gene 12 Contributes to Cell Growth and Invasion in Cervical Cancer by Acting as a Sponge for MiR-424-5p. Cell Physiol Biochem. 2018;45(5):2086-2094.
24. Wang F, Wang J, Yang X, et al. MiR-424-5p participates in esophageal squamous cell carcinoma invasion and metastasis via SMAD7 pathway mediated EMT. Diagn Pathol. 2016;11(1):88.
25. Liu J, Gu Z, Tang Y1, et al. Tumour-suppressive microRNA-424-5p directly t argets CCNE1 as potential prognostic markers in epithelial ovarian cancer. Cell Cycle. 2018;17(3):309-318.
26. Tao T, Shen Q, Luo J, et al. MicroRNA-125a Regulates Cell Proliferation Via Directly Targeting E2F2 in Osteosarcoma.Cell Physiol Biochem. 2017;43(2):768-774.
27. Xiang S, Wang Z, Ye Y, et al. E2F1 and E2F7 differentially regulate KPNA2 to promote the development of gallbladder cancer. Oncogene. 2019;38(8):1269-1281.
28. Zhao ZM, Yost SE, Hutchinson KE, et al. CCNE1 amplification is associated with poor prognosis in patients with triple negative breast cancer. BMC Cancer. 2019;19(1):96.
29. Kabakci Z, Käppeli S, Cantù C, et al. Pharmacophore-guided discovery of CDC25 inhibitors causing cell cycle arrest and tumor regression. Sci Rep. 2019;9(1):1335.
30. Zhao C, Wang XB, Zhang YH, Zhou YM, Yin Q, Yao WC. MicroRNA-424 inhibits cell migration, invasion and epithelial-mesenchymal transition in human glioma by targeting KIF23 and functions as a novel prognostic predictor. Eur Rev Med Pharmacol Sci. 2018;22(19):6369-6378.

Figures

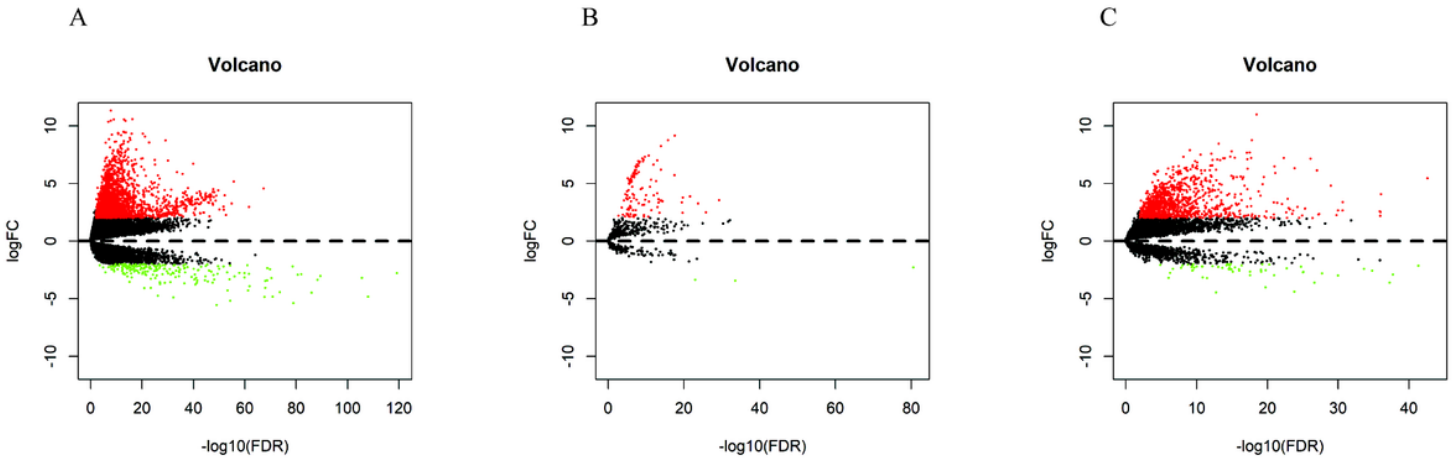

Figure 1

Volcanic maps of differentially expressed RNAs. (A) DElncRNAs, (B) DEmiRNAs, (C) DEmRNAs. red spots represent up-regulated genes, and green spots represent down regulated genes.

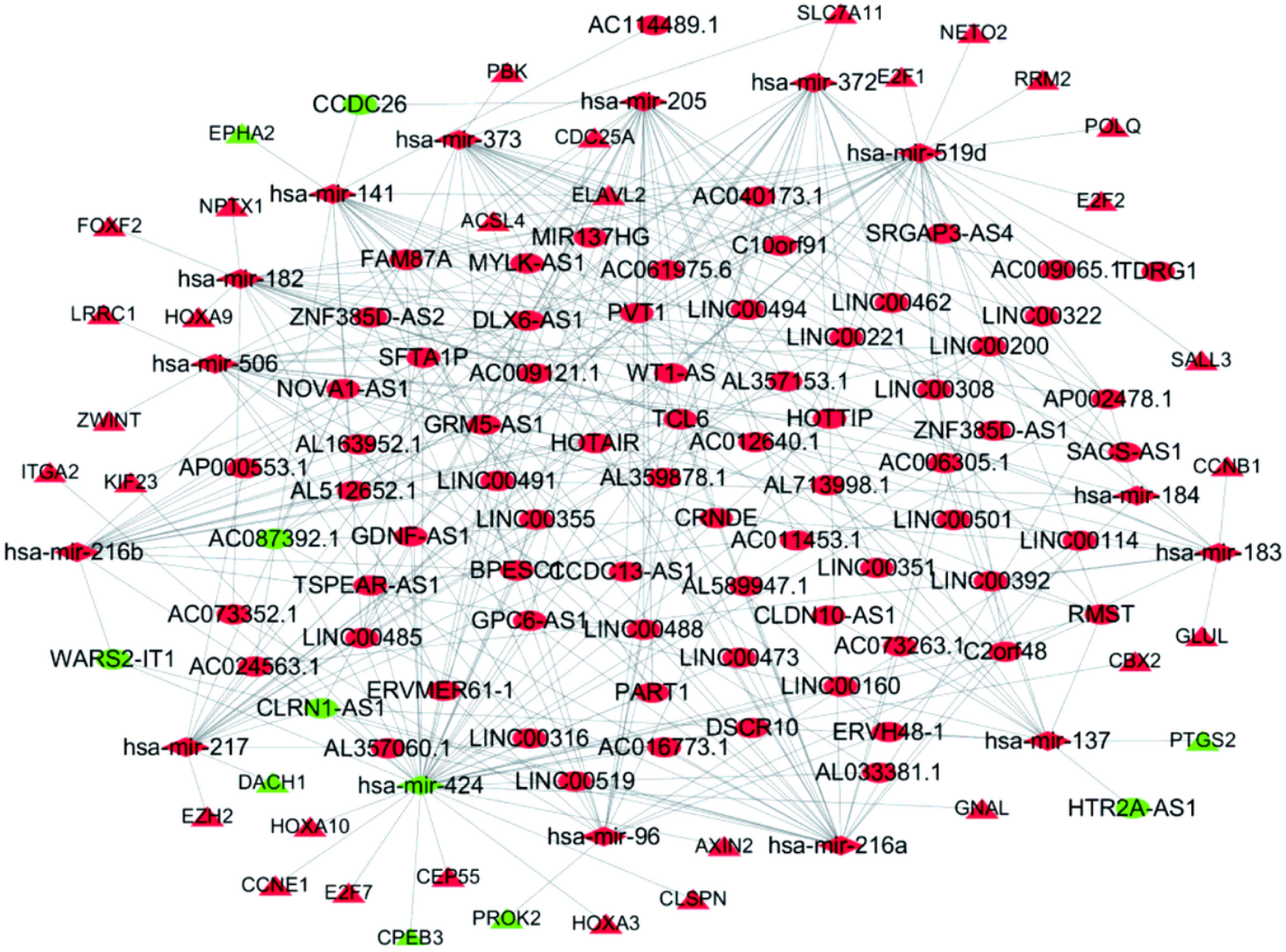

Figure 2

ceRNA regulatory network in HCC. The nodes highlighted in red indicate expression up-regulation, and the nodes highlighted in green indicate expression down-regulation. LncRNAs, miRNAs and mRNAs are represented by ellipse, diamond, triangle, respectively.

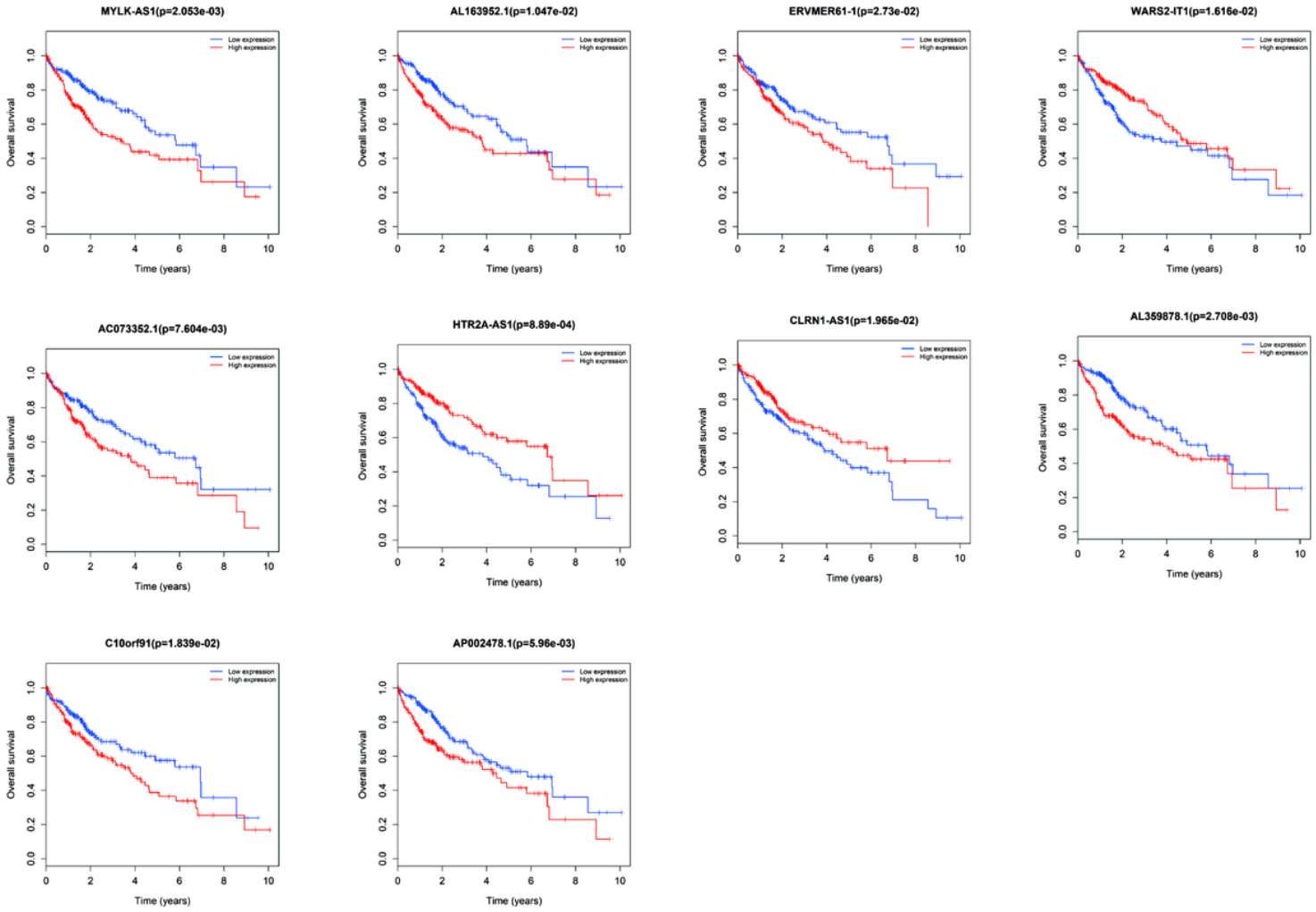

Figure 3

The most significant ten lncRNAs associated with overall survival in ceRNA network in HCC on Kaplan-Meier survival curves. The horizontal axis represents overall survival time (years), vertical axis represents survival function. ($P < 0.05$).

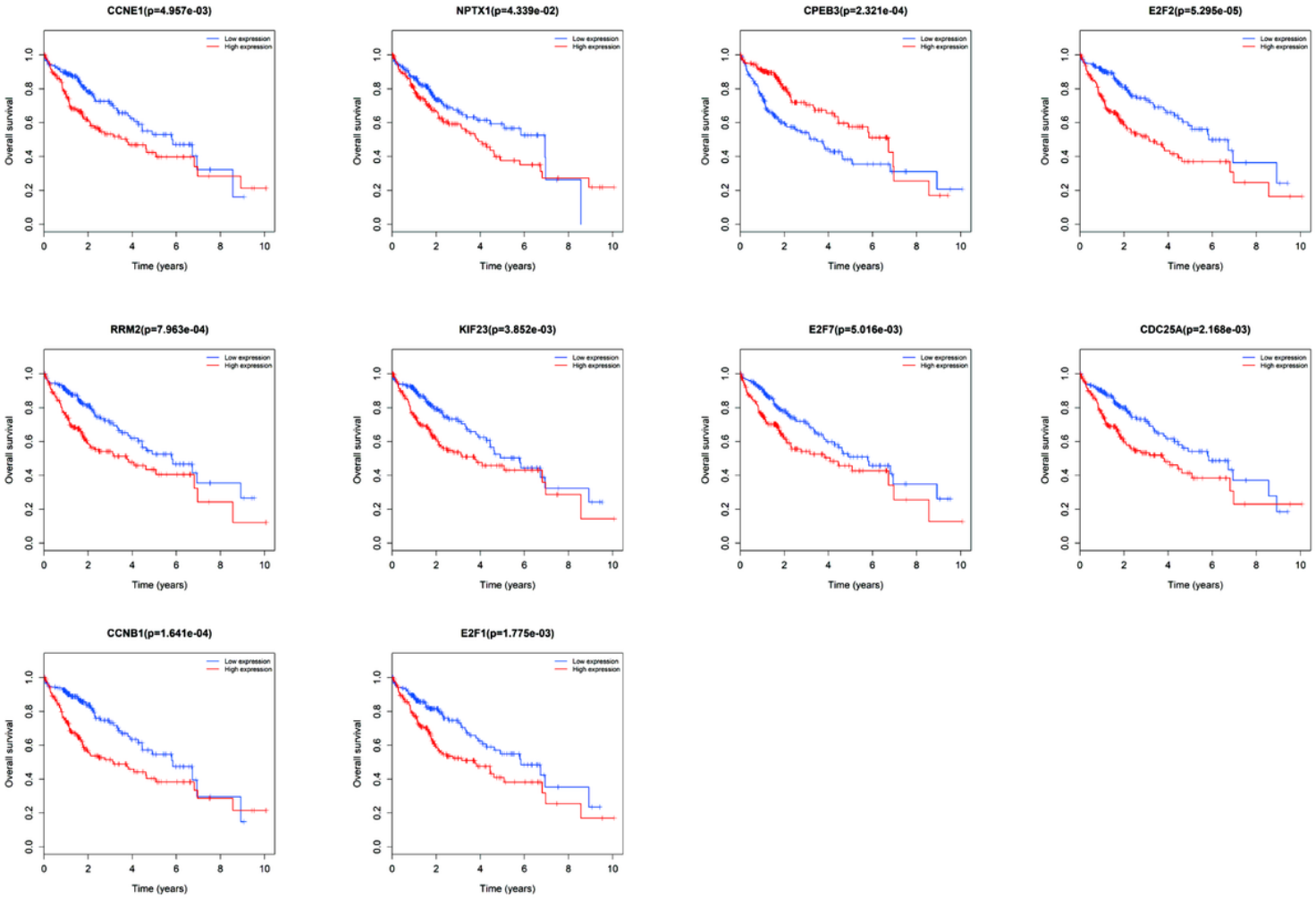

Figure 4

The most significant ten protein-coding genes associated with overall survival in ceRNA network in HCC on Kaplan-Meier survival curves. The horizontal axis represents overall survival time (years), vertical axis represents survival function. ($P < 0.05$).

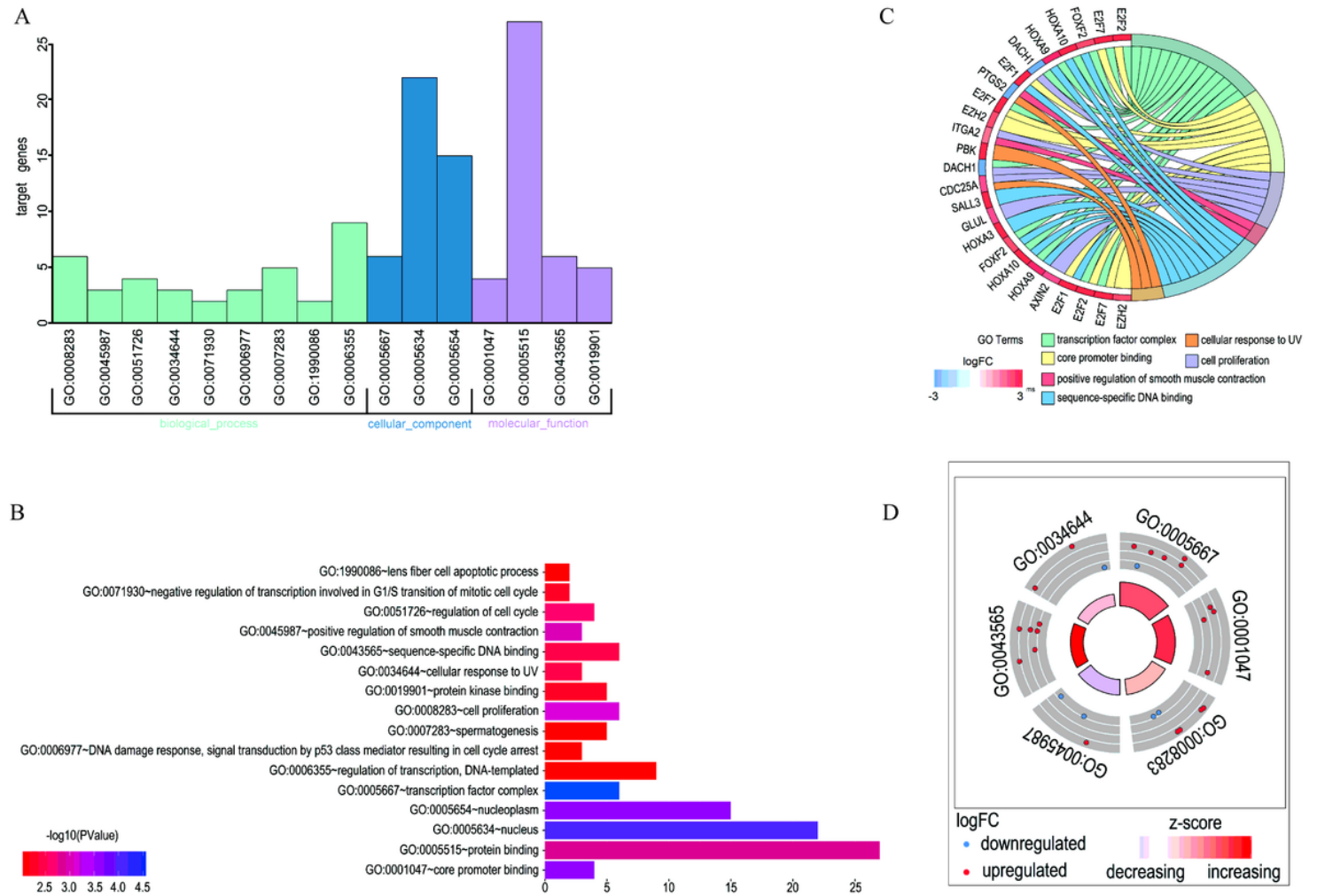

Figure 5

GO enrichments analysis of the ceRNA network. (A-B) The first 16 GO enrichments analysis with the most significant p-values.The x-axis represents the number of DEmRNAs involved in the pathway. (C-D) DEmRNAs were enriched GO pathways in HCC.

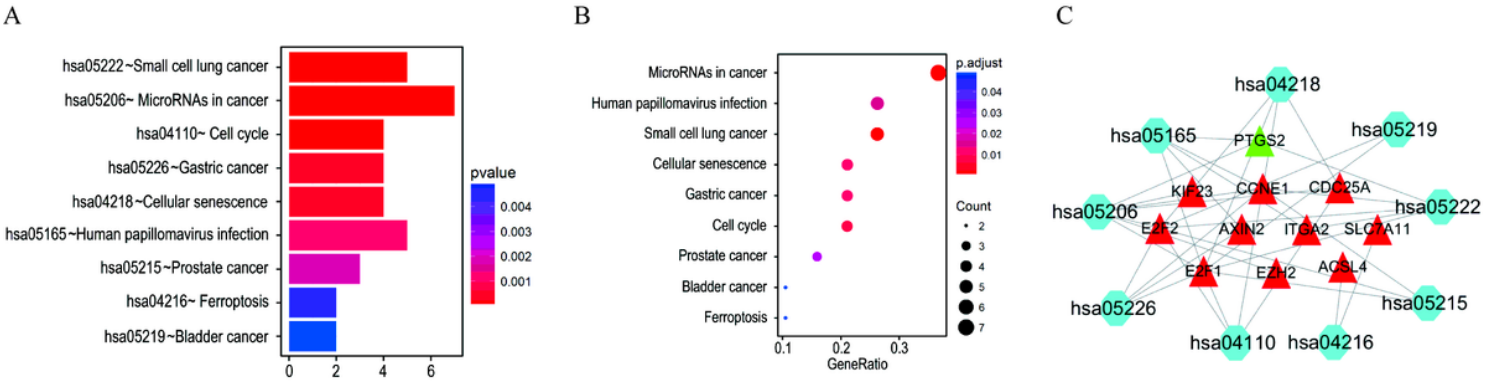

Figure 6

KEGG pathways analysis of the ceRNA network. (A-B) The top 9 KEGG pathways analysis with the most significant p-values. The x-axis represents the number of DEmRNAs involved in the pathway. (C)

DEmRNAs were enriched KEGG pathways in HCC.

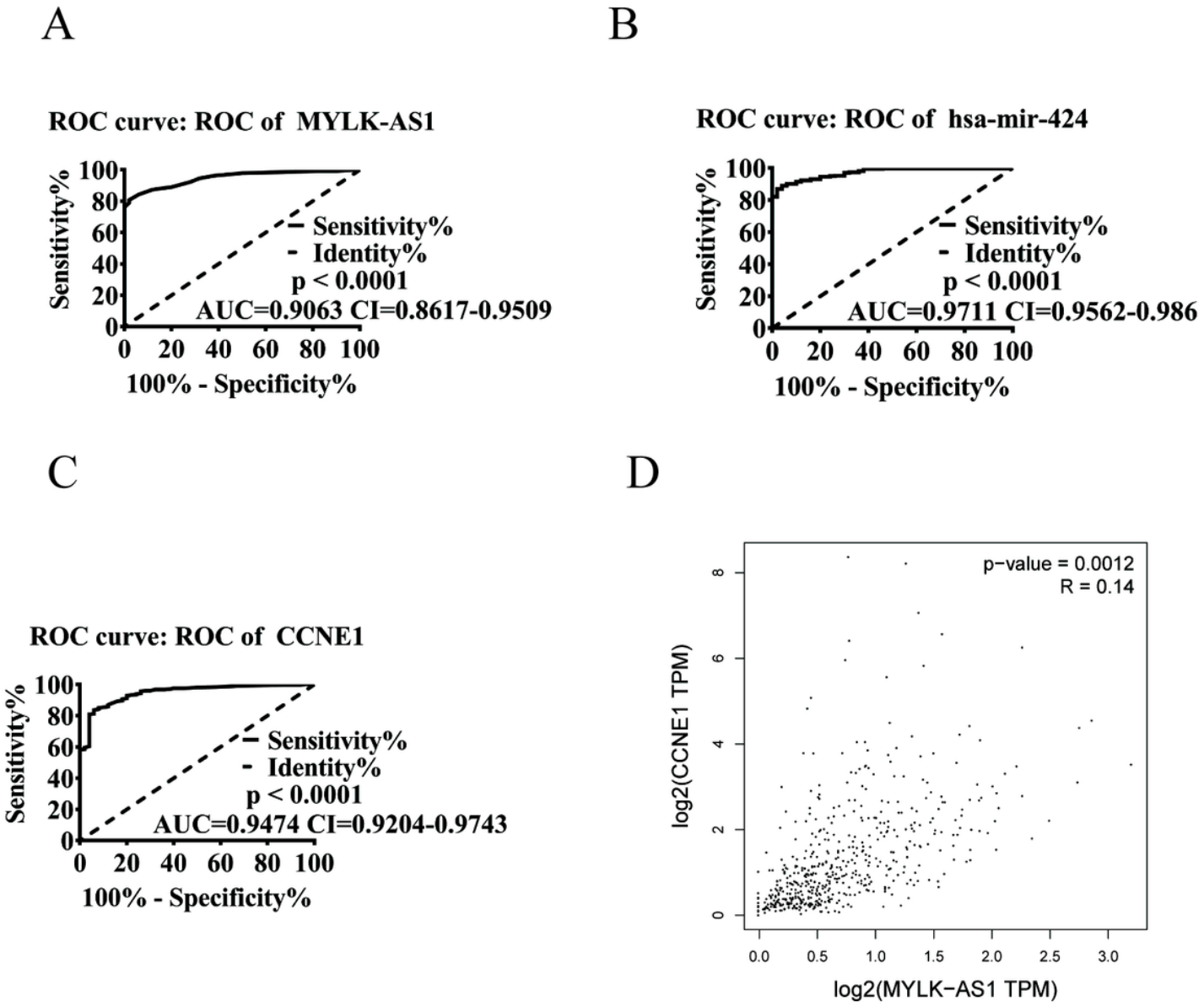

Figure 7

Prognostic value of MYLK-AS1—has-mir-424—CCNE1. (A-C) ROC curve of MYLK-AS1—has-mir-424—CCNE1 expression in HCC tissue and normal tissue from TCGA database. (D) Pearson's correlation between MYLK-AS1 and CCNE1 in TCGA database.

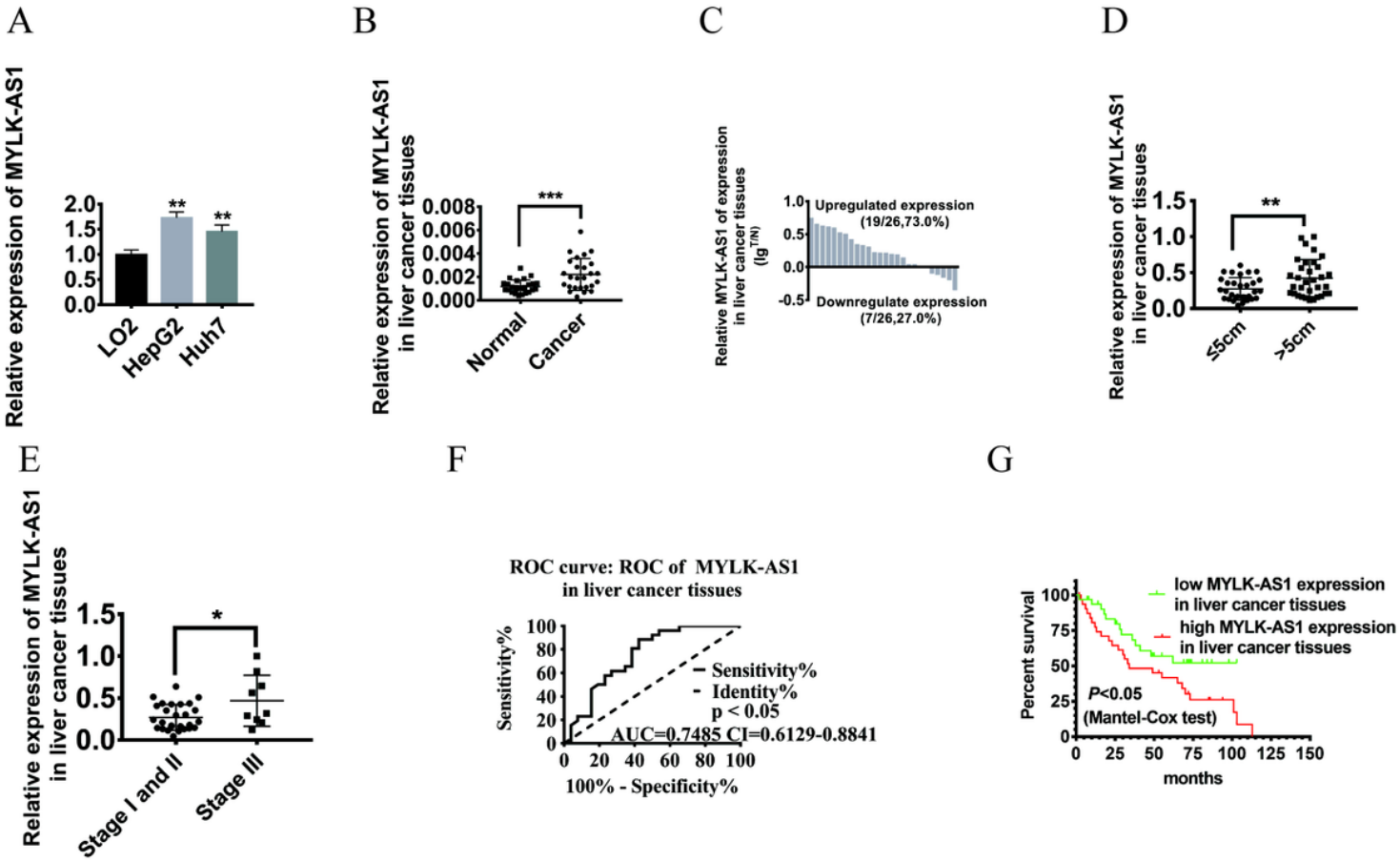

Figure 8

Differential expression of MYLK-AS1 in HCC cells and tissues . (A) MYLK-AS1 expression in HCC cells relative to normal HCC cells. (**P<0.01). (B) MYLK-AS1 expression in HCC tissue and normal tissue (***P<0.001). (C) Upregulated and downregulated expression of MYLK-AS1 in HCC tissues and normal tissues (T: tumor; N: normal). (D)Relative expression of MYLK-AS1 was examined in tumour size (**P<0.01). (E) MYLK-AS1 expression levels in different grade of HCC tissues (*P<0.05). (F) ROC curve of MALAT1 expression in HCC tissues and normal tissues. (G) Kaplan-Meier survival analysis according to MALAT1 expression level in HCC tissues and normal tissues. (*P<0.05, log rank test).

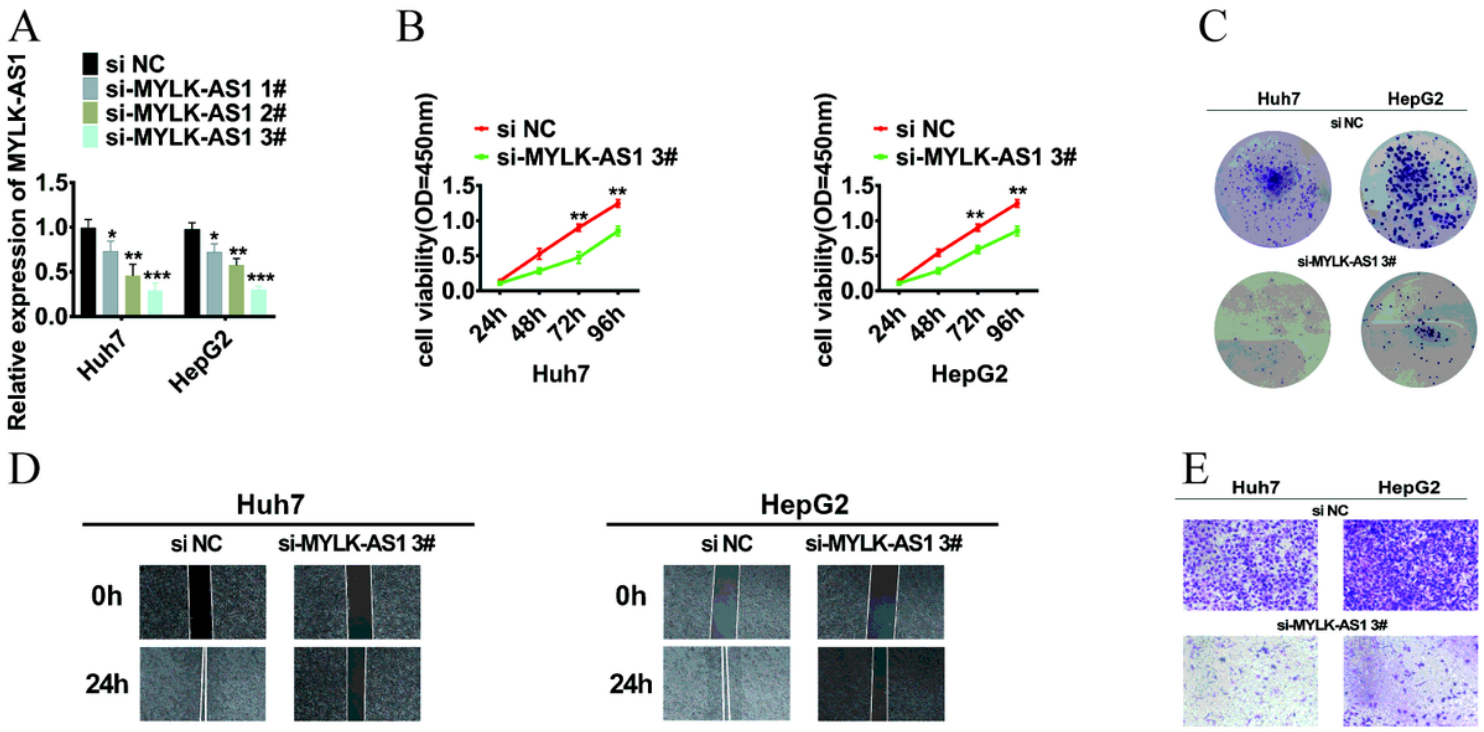

Figure 9

MYLK-AS1 silencing inhibits HCC cell proliferation (A) MYLK-AS1 levels in Huh7 and HepG2 cells after treatment with si- MYLK-AS1 1#, si-MYLK-AS1 2#, si- MYLK-AS1 3#, or si negative control (NC) by RT-PCR. (B) Cell proliferation assays after treatment with si-MYLK-AS1 3# or si NC via CCK-8 assays. (C) Colony-forming assays after treatment with si-MYLK-AS1 3#or si NC. (D) Wound healing assays after treatment with si-MYLK-AS1 3#or si NC. (E) Transwell invasion analysis after treatment with si-MYLK-AS1 3#or si NC. For all quantitative results, data are presented as the mean ± SEM from three independent experiments. *p<0.05; **p<0.01; ***P<0.001.

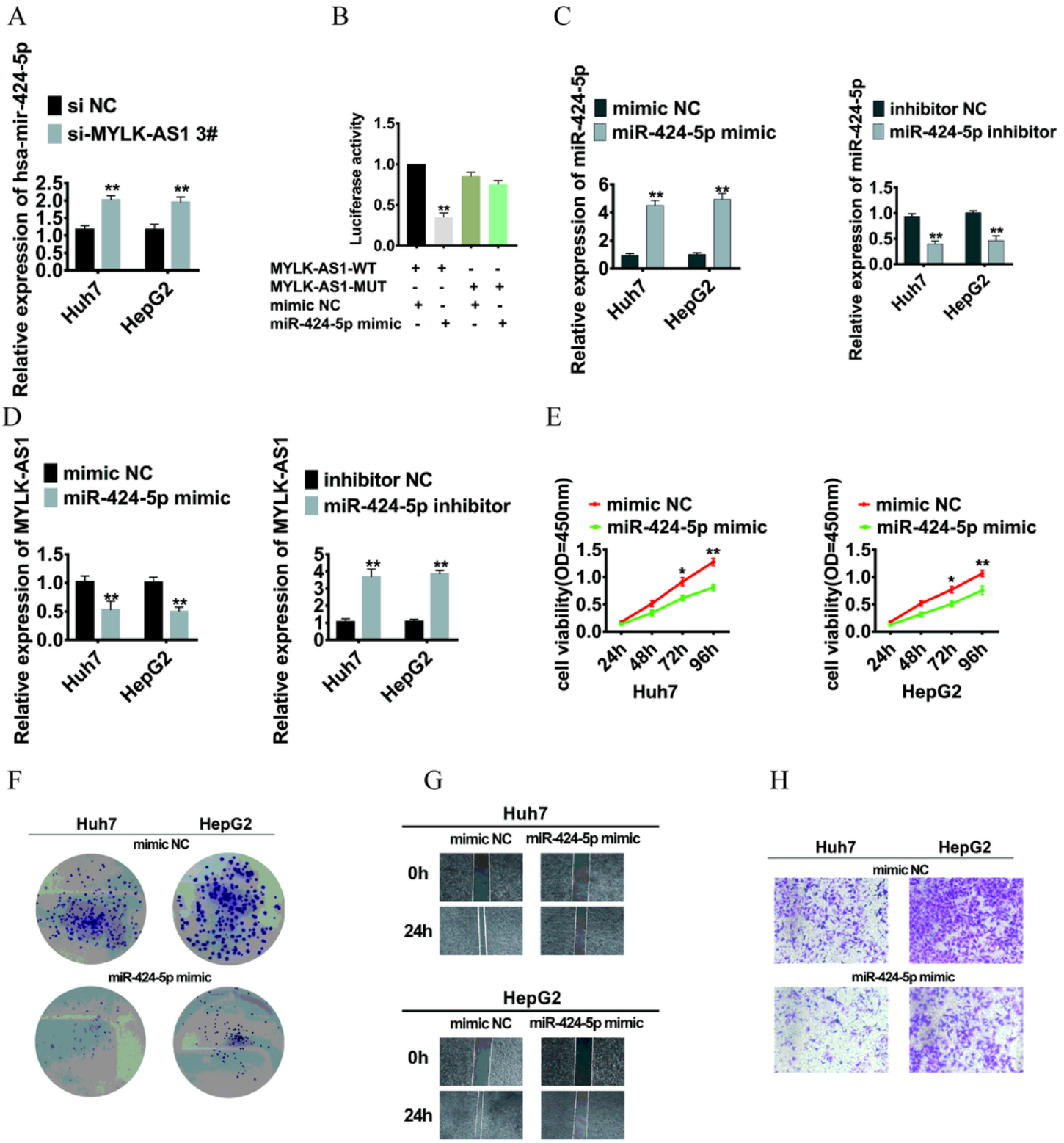

Figure 10

MYLK-AS1 functions as a ceRNA and sponges miR-424-5p in HCC cells. (A) Expression of miR-424-5p in Huh7 and HepG2 cells after treatment with si-MYLK-AS1 3#or si NC. (B) Luciferase assays in HEK-293T cells transfected with luciferase reporter plasmids containing wild type (WT) or mutant (Mut) MYLK-AS1, and mimic controls or miR-424-5p mimics. (C) miR-424-5p expression in Huh7 and HepG2 cells after treatment with miR-424-5p mimics, mimic controls, inhibitor or inhibitor control. (D) Cell proliferation

assays, (E) Colony forming assays, (F) wound healing assays, (G) Transwell invasion analysis of in Huh7 and HepG2 cells after treatment with miR-145 mimics or mimic controls. For all quantitative results, data are presented as the mean ± SEM from three independent experiments. *p<0.05; **p<0.01.

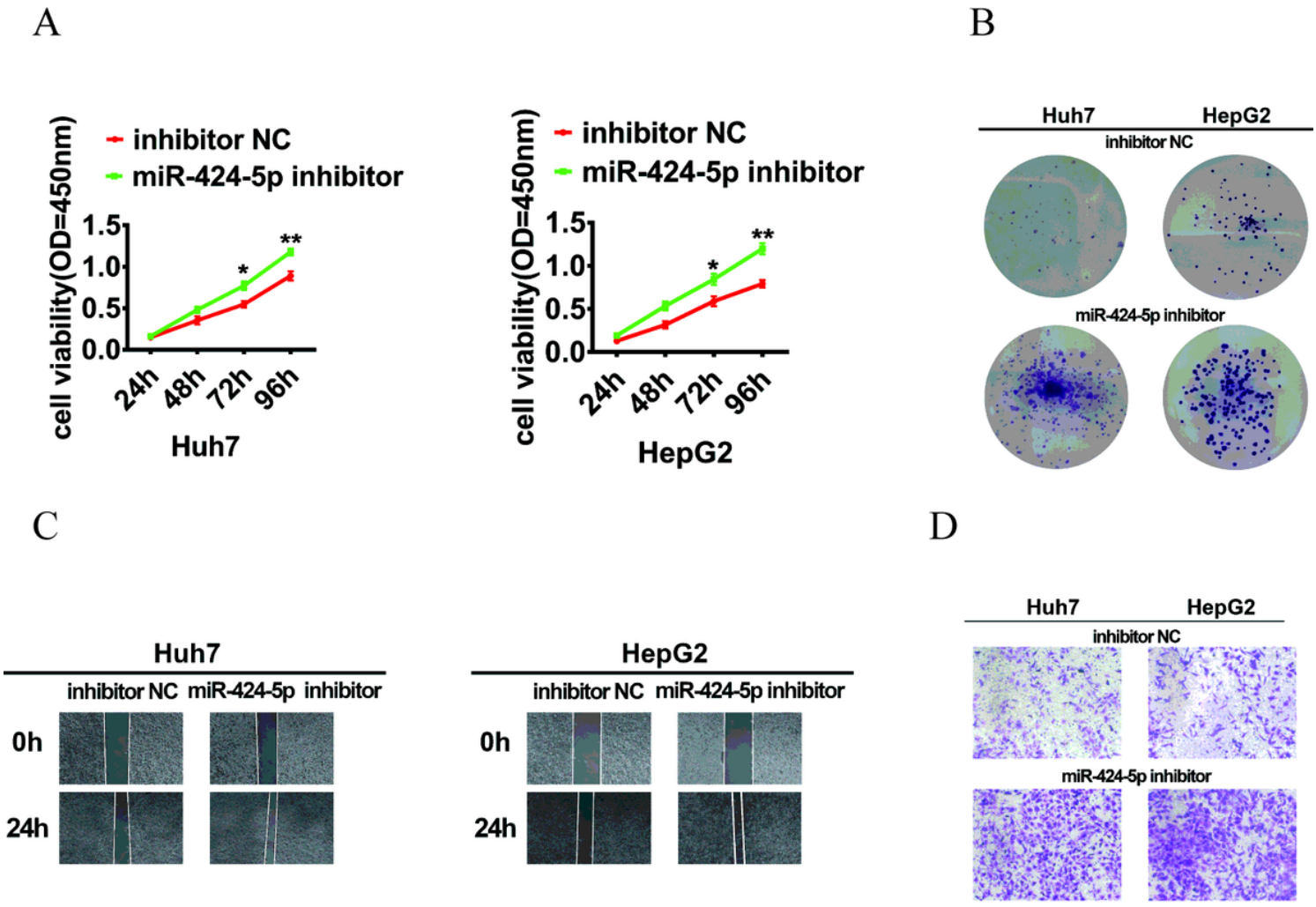

Figure 11

(A) Cell proliferation assays, (B) Colony forming assays, (C) wound healing assays, (D) Transwell invasion analysis of in Huh7 and HepG2 cells after treatment with miR-424-5p inhibitor or inhibitor controls. For all quantitative results, data are presented as the mean ± SEM from three independent experiments. *p<0.05; **p<0.01.

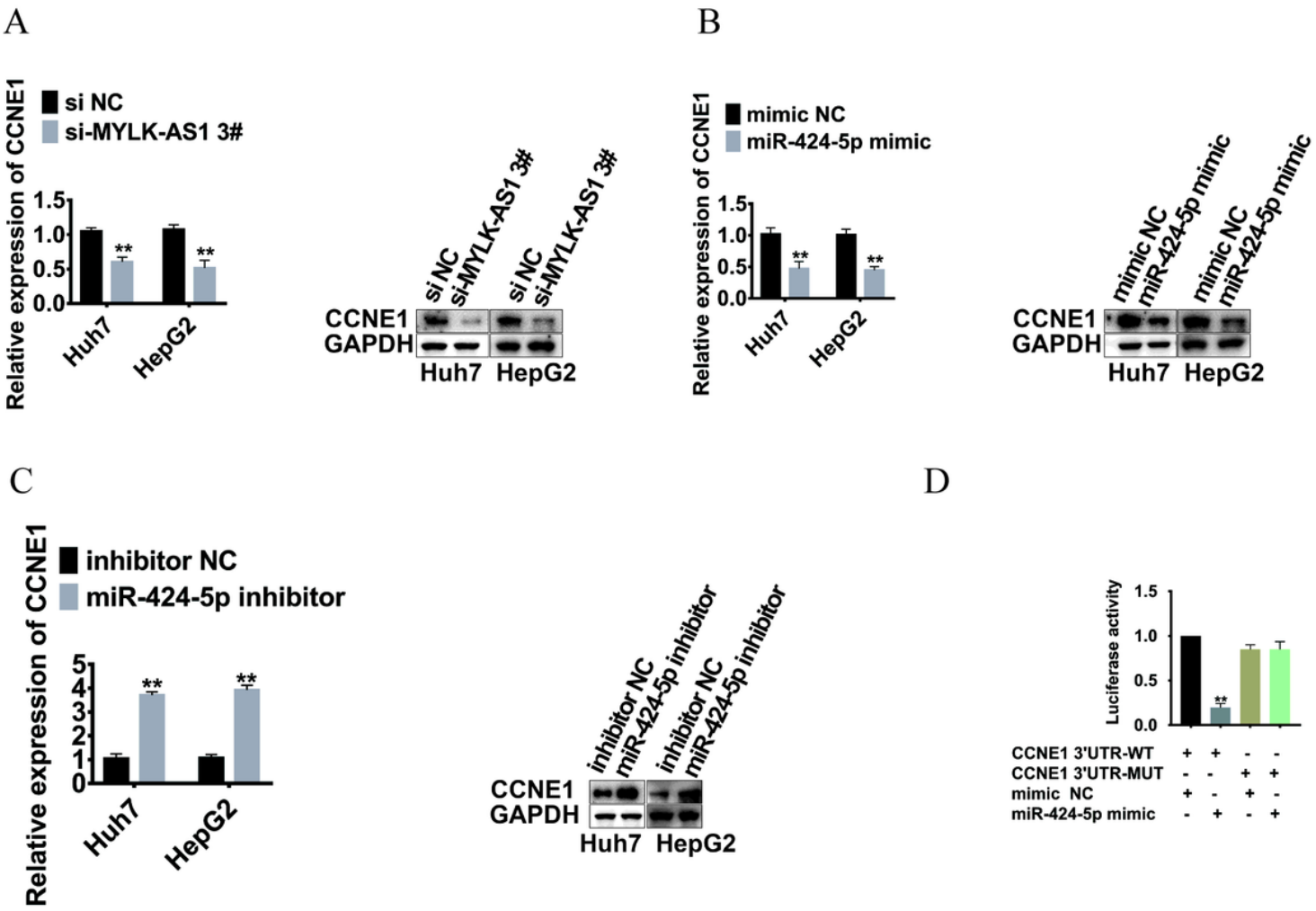

Figure 12

CCNE1 is a miR-424-5p target gene and is indirectly regulated by MYLK-AS1. (A) RT-PCR and Western blot analysis of the expression levels of CCNE1 in Huh7 and HepG2 cells transfected with si-MYLK-AS1 3#or si NC. (B) RT-PCR and Western blot analysis of the expression levels of CCNE1 in Huh7 and HepG2 cells transfected with miR-424-5p mimics, mimic controls. (C) RT-PCR and Western blot analysis of the expression levels of CCNE1 in Huh7 and HepG2 cells transfected with miR-424-5p inhibitor or inhibitor control. (E) Luciferase assays in HEK-293T cells transfected with luciferase reporter plasmids containing wild type (WT) or mutant (Mut) CCNE1 3'UTR, mimic controls; or miR-424-5p mimics. *p<0.05; **p<0.01.

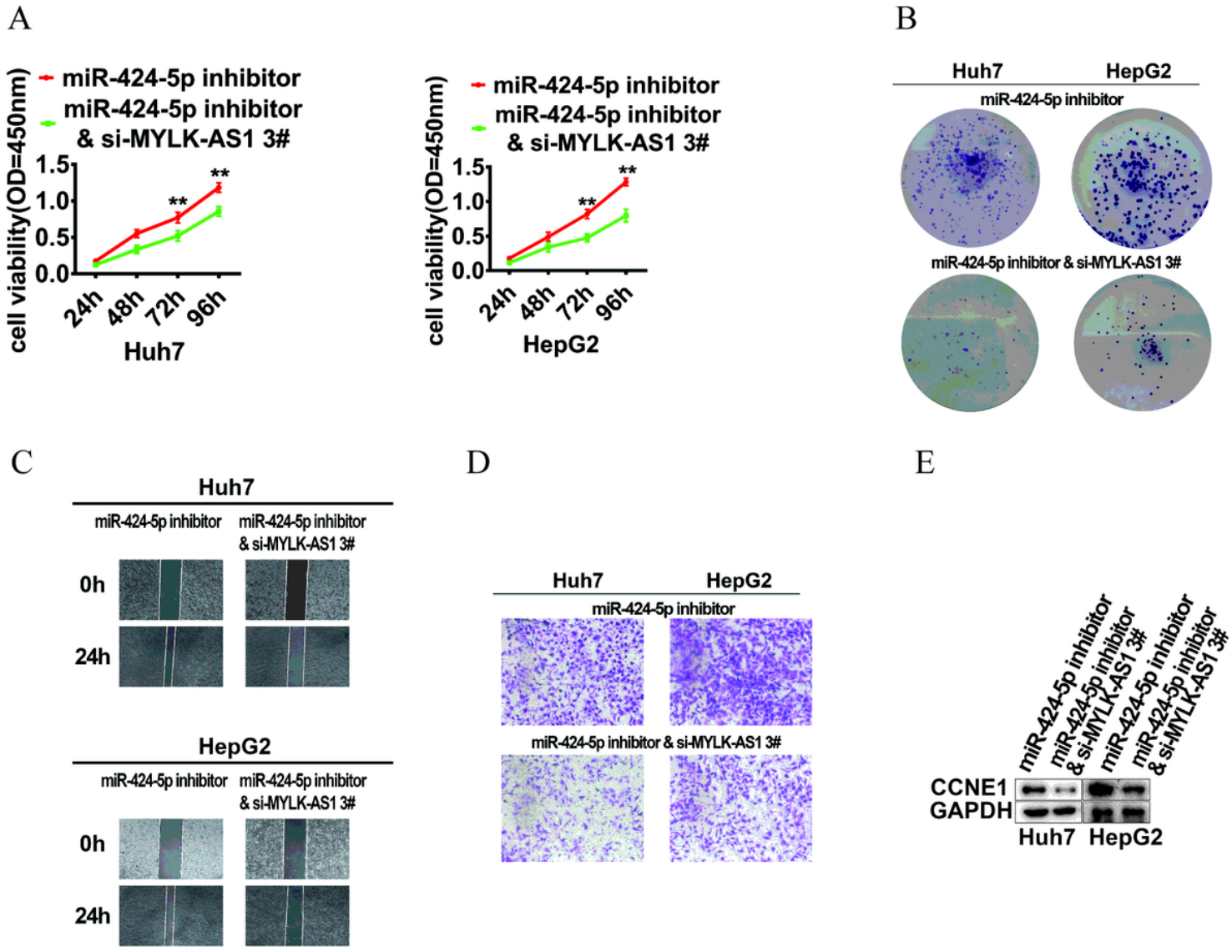

Figure 13

miR-424-5p plays a role in the relationship between MYLK-AS1 and CCNE1. (A-B) The proliferation of in Huh7 and HepG2 cells co-transfection with si-MYLK-AS1 3 #, miR-424-5p inhibitor were determined by CCK8 and colony forming assays.(C-D) Cell migration ability for Huh7 and HepG2 cells after co-transfection with si-MYLK-AS1 3 #, miR-424-5p inhibitor were determined by wound healing assay and transwell assay. (E) The expression levels of CCNE1 in Huh7 and HepG2 cells co-transfection with si-MYLK-AS1 3 #, miR-424-5p inhibitor were determined by Western blot analysis. *P<0.05; **P<0.01.

Supplementary Files

This is a list of supplementary files associated with this preprint. Click to download.

- luciferasecomplementarybindingsites.docx
- DElncRNAsTableS3.xlsx

- DEmiRNAsTableS2.xlsx
- DEmRNAsTableS1.xlsx